dynamics. An analysis of the resulting structures has been developed employing a detailed evaluation of the strain energy that is imposed by the NOE derived distance constraints.

This NOE-induced strain energy analysis is shown to be more useful in discriminating structural models developed for biphenomycin than analyses that use deviations from NOE distance bounds or torsion angles derived from J coupling as the criteria. *We conclude that the most effective criterion for the evaluation of model structures is not how closely a relaxed structure matches the distance data, but rather how much strain is induced when the structure does fit the NOE data.*

Acknowledgment. We thank Dr. Mine, Fujisawa Pharmaceutical Co., Ltd., for a sample of biphenomycin A. We are indebted to Dr. D. Hare (Hare Research Inc.) for his distance geometry program, DSPACE, and to Drs. G. M. Crippen and J. Blaney for providing modified versions of the distance geometry program.

Registry No. Biphenomycin A, 100296-21-7.

Supplementary Material Available: Total energies for the 60 structures from the DGEOM study when relaxed and when constrained (both from the local refinement and slow growth procedures using the data in Table I and from slow growth with the subset of Table I corresponding to the Kannan and Williams[3] data set), the solvent-accessible surfaces of the low-energy structures given in Table IV, and the coordinates for the *RSSS* solution conformation model (6 pages). Ordering information is given on any current masthead page.

Theoretical Studies of High-, Intermediate-, and Low-Spin Model Heme Complexes

Frank U. Axe, Charles Flowers, Gilda H. Loew,* and Ahmad Waleh*

Contribution from The Molecular Theory Laboratory, The Rockefeller University, 701 Welch Road, Suite 213, Palo Alto, California 94304. *Received February 25, 1988*

Abstract: We report here the systematic application of a semiempirical INDO/S-RHF (restricted Hartree-Fock) open-shell procedure to calculate the relative energies, electron and spin distributions, and Mössbauer quadrupole splittings for the low-lying spin states of a series of eighteen high- ($S = {}^5/_2$), intermediate- ($S = {}^3/_2$), and low-spin ($S = {}^1/_2$) ferric heme complexes for which crystal geometries are known and the ground spin states can be inferred from the observed electromagnetic properties. In general, the predicted ground spin state and the calculated energies of the other spin states relative to it are quantitatively consistent with the observed effective magnetic moments, ESR spectra, and the Mössbauer quadrupole splitting spectra for the compounds studied. For all the high-spin compounds studied, the doublet states are predicted to be thermally inaccessible, being 14-35 kcal/mol higher in energy than the sextet state. The calculated energy separation between the quartet and sextet states are significantly high in the five-coordinated compounds (~11 kcal/mol) and decreases to less than 5 kcal/mol in the six-coordinated compounds. For diaquo and diethanol ferric heme complexes, we calculate near-degenerate $S = {}^3/_2$ and $S = {}^5/_2$ states. The intermediate-spin compounds exhibit a quartet ground state, consistent with experimental observations, with an energy separation of 2-7 kcal/mol from the sextet and about 20 kcal/mol from the doublet states. The calculated results for the low-spin complexes all exhibit rather pure $S = {}^1/_2$ ground states. Only for complexes exhibiting different crystal geometries for the same axial ligands are the sextet and quartet states close enough in energy to the doublet state that interaction with these spin states of higher multiplicity may be significant. The results obtained for all complexes studied allow insights into the effect of geometry and axial ligand(s) on the relative energies and observable properties of various spin states of ferric heme complexes.

The presence of low-lying states of different multiplicities is a characteristic feature of heme active sites, as evidenced by their observed electromagnetic properties and by changes in spin states that occur during their biological function.[1-5] Studies of model heme complexes have revealed that the relative ordering of the manifold of low-lying spin states depends greatly upon the axial ligand(s) and the geometry of the complex.[6-9] A parallel dependence is also observed in intact heme proteins.[5] Therefore, theoretical identification and characterization of such spin states are very important in understanding the origin of electromagnetic properties and spectra of the heme proteins and the influence of chromophore geometry and axial ligands on their biological functions. Spin-state changes frequently occur during the biological function of heme proteins, accompanied by geometry changes or changes in axial ligands of the heme unit. Thus, it is important to establish a 1:1 correspondence between geometry, nature of axial ligand, and spin-state manifold that would allow spin to be deduced from geometry and vice versa.

We have, in the past, successfully applied[10] a semiempirical INDO/S method[11,12] to characterize the ground and excited states of various closed-shell model heme complexes. Now, by employing a restructed Hartree-Fock (RHF) and a generalized CI formalism,[13-15] the application of the INDO/S method can be ex-

* Authors to whom correspondence should be addressed.

(1) (a) Poulos, T. L. *Adv. Inorg. Biochem.* **1988**, *7*, 1-36. (b) Poulos, T. L.; Finzel, B. C. In *Peptide and Protein Reviews*; Hearn, M. T. W., Ed.; Marcel Dekker: New York, 1984; Vol. 4, p 115.
(2) Dunford, H. B.; Stillman, J. S. *Coord. Chem. Rev.* **1976**, *19*, 187.
(3) Schonbaum, G. R.; Chance, B. In *The Enzymes*, 3rd ed.; Boyer, P. D., Ed.; Academic Press: New York, 1976; pp 295-332.
(4) Hewson, W. D.; Hager, L. P. In *The Porphyrins*; Dolphin, D., Ed.; Academic Press: New York, 1979; Vol. 7, pp 295-332.
(5) Dawson, J. H.; Eble, K. S. *Advanced Inorg. Bioinorg. Mech.* **1986**, *4*, 1.
(6) Scheidt, W. R.; Reed, C. A. *Chem. Rev.* **1981**, *81*, 543.
(7) Williams, R. J. P. *Fed. Proc., Fed. Am. Soc. Exp. Biol.* **1961**, *20*, 5.
(8) Hoard, J. L.; Hamor, M. J.; Hamor, T. A.; Caughey, W. S. *J. Am. Chem. Soc.* **1965**, 2312.
(9) Hoard, J. L. *Science* **1971**, *174*, 1295.
(10) Loew, G. H. In *Iron Porphyrins, Part I*; Lever, A. B. P., Gray, H. B., Eds.; Addison-Wesley: Reading, MA, 1983; pp 1-87.
(11) Ridley, J.; Zerner, M. *Theor. Chim. Acta* **1973**, *32*, 111. Ridley, J. E.; Zerner, M. C. *Theor. Chim. Acta* **1976**, *42*, 223. Bacon, A. D.; Zerner, M. C. *Theor. Chim. Acta* **1979**, *53*, 21.
(12) Zerner, M. C.; Loew, G. H.; Kirchner, R. F.; Muller-Westerhoff, U. T. *J. Am. Chem. Soc.* **1980**, *102*, 589.
(13) Edwards, W. D.; Zerner, M. C. *Theor. Chim. Acta* **1987**, *72*, 347.

0002-7863/89/1511-7333$01.50/0

tended[16,17] to all hemeprotein complexes independent of their oxidation and spin states. However, given the approximate nature of the semiempirical methods, an even-handed and reliable prediction of the spin states and the associated electronic and electromagnetic properties in hemeprotein requires a systematic calibration and test of the method in systems for which crystal geometries are known and the electromagnetic properties are reasonably inferred from experiments.

Fortunately, the structures of a variety of five- and six-coordinated model ferric heme complexes have been characterized by X-ray diffraction[18-35] techniques. Furthermore, Mössbauer resonance,[23,25,26,29-31,36-41] magnetic susceptibility,[22-26,28-32,34,35,37,39,42,43] and electron spin resonance (ESR) spectra[28,29] have been measured for many of these compounds and/or their analogues. Some ferric complexes display properties that are characteristic of one predominant ground spin state. Others display large zero-field splittings, temperature-dependent magnetic moments, or highly anisotropic ESR g values which indicate contributions from more than one dominant spin state.[43-48] These deviations in the electromagnetic properties from the values expected for pure spin states have been interpreted in terms of either a thermal equilibrium between pure, noninteracting $S = {}^5/_2$ and $S = {}^1/_2$ spin states[49] or a quantum mechanical mixture of low-lying quartet and sextet states,[48] through spin–orbit coupling. Mixing of both sextet and quartet spin states with a doublet state has also been suggested from the optimization of ligand-field parameters to account for the observed magnetic properties of ferric heme complexes.[43-47]

Synthesis of model ferric complexes has shown that different crystal geometries can be obtained with the same axial ligands,[29,35] resulting in different relative mixing of spin states. For example, both monoclinic[29] and triclinic[35] crystal forms of $[Fe(OEP)(3\text{-}ClPy)_2]ClO_4$ have been isolated, which on the basis of magnetic susceptibility and Mössbauer data have been characterized as a quantum-admixed intermediate-spin[29] and a low-spin[35] complex, respectively. Similarly, two crystal forms of [Fe(OEP)(NCS)(Py)] and [Fe(TPP)(NCS)(Py)] are reported to be high-spin ($S = {}^5/_2$) and low-spin ($S = {}^1/_2$) complexes, respectively.[24]

In this paper, we report the results of a systematic investigation of the effect of geometry and axial ligand(s) on the relative energies of the low-lying spin states and the calculations of quadrupole splitting, ΔE_Q, for 18 model ferric heme complexes. This study represents a test of the capabilities of the INDO/S-RHF method to identify and predict the ground spin state and the electronic properties of iron porphyrin complexes and hemeprotein active sites. The ferric heme complexes used in this study include a representative number of high-, intermediate-, and low-spin systems for which crystal geometries are available. The unbiased frozen-crystal-geometry calculations of the relative energies of various spin states should provide important information about the relationship between geometry and spin and the role of axial ligands in stabilizing a particular spin state.

Methods

All calculations were carried out using an INDO/S (intermediate neglect of differential overlap) program that includes parametrization for transition metals. A restricted Hartree–Fock (RHF) formalism, developed by Zerner et al.,[13] was employed to quantitatively evaluate the relative spin-state energies. This program has been used successfully to study the low-lying spin states of ferrous porphine,[14] ferrous nitrosylheme,[16] ferric chlorohemin,[15] and ferric cytochrome P450 complexes.[17]

The iron–porphyrin–ligand geometries for each complex were taken directly from the X-ray crystal coordinates.[18-35] However, the peripheral substituents on the porphyrin ring were replaced by hydrogens, thus making the porphyrin a porphine model. All C–H bond lengths were assumed to be 1.08 Å and were oriented ideally according to whether the hybridization at the atom they are attached to was sp^2 or sp^3.

Energies of the lowest lying sextet, quartet, and doublet states were calculated for each of the 18 complexes studied. The d orbital configurations corresponding to the lowest energy spin states were $(d_{xy})^2(d_{xz},d_{yz})^3$ for the doublet, $(d_{xy})^2(d_{xz})^1(d_{yz})^1(d_{z^2})^1$, for the quartet, and $(d_{xy})^1(d_{xz})^1(d_{yz})^1(d_{z^2})^1(d_{x^2-y^2})^1$ for the sextet states. The notation corresponds to the orientation of the porphyrin macrocycle being in the xy plane with the pyrrole nitrogens placed, as nearly as possible, on the x and y axes. The sextet-state configuration is unique. The choice of the lowest energy configurations for the doublet and quartet states was confirmed by calculating various quartet and doublet configurations, obtained by assigning the unpaired electron(s) to different iron d orbitals, in some representative number of complexes. They are also corroborated by a recent detailed study of chlorohemin.[15]

The quadrupole splitting, ΔE_Q, for each complex was calculated from the INDO-RHF eigenvectors. This quantity is determined by first calculating the nine components (V_{ij}) of the electric field gradient tensor by using an appropriate one-electron operator and the spin density matrix, taking into account only the iron d-orbital contributions over all the singly and doubly occupied orbitals. The resulting 3 × 3 electric field gradient tensor is then diagonalized, and the principal values are ordered as $|V_{ii}| > |V_{jj}| > |V_{kk}|$. These values are then used in the expression

$$\Delta E_Q = \delta(1 - R)Qq[1 + \eta^2/3]^{1/2} \quad (1)$$

where $q = V_{ii}$, $\eta = (V_{kk} - V_{jj})/V_{ii}$ $(0 \le \eta < 1)$, $(1 - R)$ = Sternheimer shielding constant, and Q = nuclear quadrupole moment. The sign of ΔE_Q is the sign of the largest field gradient component, V_{ii}. Values of Q and $(1 - R)$ used in these calculations are 0.187 and 0.68, respectively. As discussed in the text, the coefficient δ is equal to 1 for low-spin and 2 for both high- and intermediate-spin complexes.

Results

Table I shows the calculated relative energies in kcal/mol for the $S = {}^5/_2$, ${}^3/_2$, and ${}^1/_2$ spin states for the crystal geometries of

(14) Edwards, W. D.; Weiner, B.; Zerner, M. C. *J. Am. Chem. Soc.* **1986**, *108*, 2196.
(15) Edwards, W. D.; Weiner, B.; Zerner, M. C. *J. Phys. Chem.*, in press.
(16) Waleh, A.; Ho, N.; Chantrannpong, L.; Loew, G. H. *J. Am. Chem. Soc.*, in press.
(17) Waleh, A.; Collins, J. R.; Loew, G. H.; Zerner, M. C. *Int. J. Quantum Chem.* **1986**, *29*, 1575.
(18) Sabat, M.; Ibers, J. A. *J. Am. Chem. Soc.* **1982**, *104*, 3715.
(19) Koenig, D. F. *Acta Crystallogr.* **1965**, *18*, 663.
(20) Anzai, K.; Hatano, K.; Lee, Y. J.; Scheidt, W. R. *Inorg. Chem.* **1981**, *20*, 2337.
(21) Skelton, B. W.; White, A. H. *Aust. J. Chem.* **1977**, *30*, 2655.
(22) Phillippi, M. A.; Baenziger, N.; Goff, H. *Inorg. Chem.* **1981**, *20*, 3904.
(23) Tang, S. C.; Koch, S.; Papefthymiou, G. C.; Foner, S.; Frankel, R. B.; Ibers, J. A.; Holm, R. H. *J. Am. Chem. Soc.* **1976**, *98*, 2414.
(24) Scheidt, W. R.; Lee, Y. J.; Geiger, D. K.; Taylor, K.; Hatano, K. *J. Am. Chem. Soc.* **1982**, *104*, 3367.
(25) Mashiko, T.; Kastner, M. E.; Spartalin, K.; Scheidt, W. R.; Reed, C. A. *J. Am. Chem. Soc.* **1978**, *100*, 6354.
(26) Scheidt, W. R.; Cohen, I. A.; Kastner, M. E. *Biochem.* **1979**, *18*, 3546.
(27) Einstein, F. W. B.; Willis, A. *Inorg. Chem.* **1978**, *17*, 3040.
(28) Reed, C. A.; Mashiko, T.; Bently, S. P.; Kastner, M. E.; Scheidt, W. R.; Spartalian, K.; Lang, G. *J. Am. Chem. Soc.* **1979**, *101*, 2948.
(29) Scheidt, W. R.; Geiger, D. K.; Hayes, R. G.; Lang, G. *J. Am. Chem. Soc.* **1983**, *105*, 2625.
(30) Masuda, H.; Taga, T.; Osaki, K.; Sugimoto, H.; Yoshida, Z.; Ogoshi, H. *Bull. Chem. Soc. Jpn.* **1982**, *55*, 3891.
(31) Scheidt, W. R.; Haller, K. J.; Hatano, K. *J. Am. Chem. Soc.* **1980**, *102*, 3017.
(32) Scheidt, W. R.; Lee, Y. J.; Lnangdilok, W.; Haller, K. J.; Anzai, K.; Hatano, K. *Inorg. Chem.* **1983**, *22*, 1516.
(33) Inniss, D.; Soltis, M.; Stronse, C. *J. Am. Chem. Soc.* **1988**, *110*, 5644.
(34) Adams, K. M.; Rasmussen, P. G.; Scheidt, W. R.; Hatano, D. *Inorg. Chem.* **1979**, *18*, 1892.
(35) Scheidt, W. R.; Geiger, D. K.; Haller, K. J. *J. Am. Chem. Soc.* **1982**, *104*, 495.
(36) Maricondi, C.; Straub, D. K.; Epstein, L. M. *J. Am. Chem. Soc.* **1972**, *94*, 4157.
(37) Gans, P.; Buisson, G.; Duee, E.; Regnand, J. R.; Manchon, J. C. *J. Chem. Soc., Chem. Commun.* **1979**, 393.
(38) Dolphin, D. H.; Sams, J. R.; Tsin, T. B. *Inorg. Chem.* **1977**, *16*, 711.
(39) Mitra, S.; Date, S. K.; Nipankar, S. V.; Birdy, R.; Girerd, J. J. *Proc. Indian Acad. Sci.* **1980**, *89*, 511.
(40) Spartalian, K.; Lang, G.; Reed, C. A. *J. Chem. Phys.* **1979**, *71*, 1832.
(41) Rhynard, D.; Lang, G.; Spartalian, K. *J. Chem. Phys.* **1979**, *71*, 3715.
(42) Maricondi, C.; Swift, W.; Straub, D. K. *J. Am. Chem. Soc.* **1969**, *91*, 5205.
(43) Gregson, A. K. *Inorg. Chem.* **1981**, *20*, 81.
(44) Harris, G. M. *Phys. Rev.* **1966**, *149*, 198.
(45) Harris, G. *J. Chem. Phys.* **1968**, *48*, 2191.
(46) Harris, G. *Theor. Chim. Acta* **1968**, *10*, 119.
(47) Harris, G. *Theor. Chim. Acta* **1968**, *10*, 155.
(48) Maltempo, M. M.; Moss, T. H. *Q. Rev. Biophys.* **1976**, *9*, 181.
(49) Griffith, J. S. *Proc. R. Soc. London, Ser. A* **1956**, *253*, 23.

all model ferric heme complexes studied. The division of the complexes into high-, intermediate-, and low-spin reflects only the commonly accepted assignment of their spin state. For convenience, this formal spin state is used as reference, and the energies of the other two spin states are given relative to this state. Although porphyrin substituents are replaced by hydrogens in our calculation, these substituents are included in the list of the complexes to reflect the formula of the crystal structure from which the geometry was taken. Table I also shows the calculated quadrupole splitting, ΔE_Q, and the asymmetry parameter, μ, for the relevant spin state of each complex. The observed values of ΔE_Q and the net effective magnetic moment for either the same complex or a close analogue of it (indicated in the footnotes), where available, are also given for comparison.

Since calculations of the spin states correspond to a frozen crystal geometry, in instances where different crystallographic forms or crystal geometries for the same two axial ligands result in different spin states, each case is listed according to the spin state inferred from the observed properties for that geometry. Accordingly, [Fe(OEP)(NCS)(Py)] is listed among the high-spin, $[Fe(OEP)(3\text{-}ClPy)_2]_{monoclinic}^+$ among the intermediate-spin, and $[Fe(OEP)(3\text{-}ClPy)_2]_{triclinic}^+$ and [Fe(TPP)(NCS)Py] among the low-spin complexes.

Table II gives the calculated open-shell and closed-shell electron populations of the iron d orbitals. The open-shell population represents the unpaired spin density, and the sum of the open- and closed-shell populations corresponds to the total electron density in each orbital. Deviations of the spin densities (open-shell population) from unity in the iron d_{z^2} and $d_{x^2-y^2}$ orbitals for the sextet and d_{z^2} orbital for the quartet states usually indicate the extent of spin delocalization from these orbitals. Similarly, deviations of the closed-shell populations from the "ionic" limit of zero indicate the extent to which each orbital is the recipient of electrons from the axial ligand(s) and/or porphyrin ring. Table III displays the calculated Mulliken[50] net charges and unpaired spin densities on the iron, axial ligand(s), and the porphyrin ring for each complex.

The quadrupole splitting, ΔE_Q, observed in Mössbauer resonance spectra is an important indicator of the spin state of heme complexes. However, as shown in eq 1, the numerical values for ΔE_Q are determined not only by the calculated electric field gradient around the iron nucleus but also by the choice of the Sternheimer factor and the nuclear quadrupole moment. The numerical values used for these factors vary over a wide range in the literature. Previous calculations of ΔE_Q in our laboratory, using values indicated in the Methods section, have resulted in good numerical agreement between the calculated and observed values of ΔE_Q for the closed-shell ferrous heme complexes[51] and the UHF treatment of the higher iron oxidation state in HRP compound I.[52] The present study represents the first time the RHF wave functions of open-shell ferric heme systems are used in a systematic calculation of ΔE_Q. We have found that, while the calculated ΔE_Q's for the low-spin complexes are generally in agreement with the observed values, those calculated for the intermediate- and high-spin complexes are systematically lower. However, as shown in Figure 1, the correlation between the calculated and observed values is linear for the complexes studied, and the ratios of the observed ΔE_Q's, which should be independent of constant factors, are rather well reproduced by the calculations. We tentatively attribute the systematically lower values of the calculated ΔE_Q's for the intermediate- and high-spin complexes to a subtle imbalance in the net electron occupancy of the d_{z^2} and $d_{x^2-y^2}$ orbitals, resulting in lower deviations from spherical symmetry, in the determination of the electric field gradient. The linearity of the correlation in Figure 1, however, suggests a correction factor in eq 1 of $\delta = 2$ for all intermediate- and high-spin[53] complexes and a value of $\delta = 1$ for the low-spin ferric heme complexes. Accordingly, the ΔE_Q values reported in Table I are corrected by these factors.

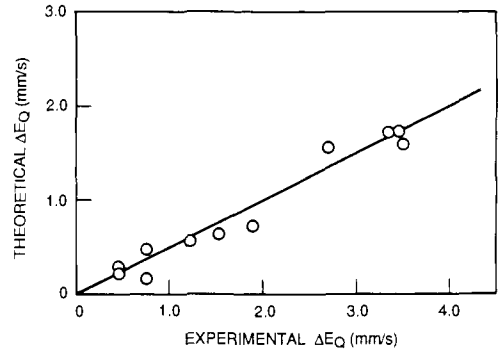

Figure 1. Calculated Mössbauer quadrupole splitting, ΔE_Q, vs experimentally observed values for intermediate- and high-spin ferric heme complexes. The solid line corresponds to $\delta = 2$ in eq 1.

Discussion

High-Spin Complexes. The results in Table I show that the sextet state is indeed the ground state in all the five-coordinate high-spin complexes, and it is definitively more stable than either the doublet or the quartet state by an average of ~30 and ~12 kcal/mol, respectively. These results are consistent with the observed effective magnetic moments of 5.90–5.94 μ_b[23,42] for these compounds, indicating a pure high-spin ground state. The calculated ΔE_Q of 0.44 mm/s for [Fe(C_2-Cap)Cl] and 0.56 mm/s for [Fe(PPIX)Cl] are in good agreement with the observed[36] value of 0.46 mm/s for [Fe(TPP)Cl]. No measured values of μ_{eff} or ΔE_Q have been reported for the fluoride complex. The calculated value of ΔE_Q for the bromide complex is anomalously low and may be the result of the bromine parameters.

Table II shows that, in the five-coordinate high-spin compounds, the d_{xy}, d_{xz}, and d_{yz} orbitals, with open-shell populations near one and closed-shell populations near zero, contribute very little to the spin delocalization and have no significant electron density donation from either the axial ligands or the porphyrin. By contrast, the $d_{x^2-y^2}$ orbital contributes significantly to the spin delocalization on the porphyrin ring. As shown in Table III, the total unpaired electron density on the porphyrin ring is about 0.5 electron for these compounds. Similarly, the d_{z^2} orbital contributes to the spin delocalization on the axial ligand. Both d_{z^2} and $d_{x^2-y^2}$ orbitals are also recipients of substantial forward donation of electron density from both the axial ligand and the porphyrin ring, as shown by the significant closed-shell populations of these two orbitals (Table II) and the reduced net formal charge on the ferric ion (Table III).

In contrast to the five-coordinate compounds, the high-spin complexes with two axial ligands exhibit a significant stabilization of the quartet and doublet spin states. Indeed, the calculated energy of the quartet state is only about 5 kcal/mol above that of the sextet state in the [Fe(OEP)(NCS)(Py)] and $[Fe(TPP)(TMSO)_2]^+$ complexes, and the two spin states are predicted to be near degenerate for the diaquo and diethanol complexes. The energy differences between the sextet and doublet states, however, are still in a range of +14 to +18 kcal/mol. Although this is significantly reduced from the ~30 kcal/mol calculated for the five-coordinate complexes, it is still too large to indicate a significant role for the doublet state in determining the observed electromagnetic properties of the six-coordinate compounds.

The smaller energy separation between the $S = {}^3/_2$ and $S = {}^5/_2$ spin states shows the potential importance of the quartet state in the six-coordinate complexes and is reflected in the interaction of the $d_{x^2-y^2}$ and d_{z^2} orbital[6] with the porphyrin ring and axial ligands. As shown in Tables II and III, with the exception of [Fe(OEP)(NCS)(Py)], the six-coordinate high-spin complexes exhibit a significantly higher electron donation (increased closed-shell population) and spin delocalization (decreased open-shell population) between the $d_{x^2-y^2}$ and porphyrin ring and a lower d_{z^2} orbital interaction with the axial ligands than in the

(50) Mulliken, R. S. *J. Chem. Phys.* **1955**, *23*, 2338.
(51) Herman, Z. S.; Loew, G. H. *J. Am. Chem. Soc.* **1980**, *102*, 1815.
(52) Loew, G. H.; Herman, Z. S. *J. Am. Chem. Soc.* **1980**, *102*, 6173.
(53) A least-squares fit of the experimental versus calculated Mössbauer splittings yielded an actual slope of 2.07.

Table I. Calculated Relative Energies and Mössbauer Parameters for the High-, Intermediate-, and Low-Spin Ferric Complexes

compound	spin	calcd ΔE, kcal/mol	calcd ΔE_Q,[gg] mm/s	calcd η	obsd E_Q(T),[gg] mm/s	obsd μ_{eff} (T), μ_b
High-Spin Complexes						
[Fe(C_2-Cap)Cl][a]	$^1/_2$	+32.6	2.75			
	$^3/_2$	+11.9	2.16			
	$^5/_2$	0.0	0.44	0.85	0.46[b] (4 K)	5.92[c] (200 K)
[Fe(PPIX)Cl][d]	$^1/_2$	+32.3	2.73			
	$^3/_2$	+12.1	1.64			
	$^5/_2$	0.0	0.56	0.96	0.46[b] (4 K)	5.92[c] (200 K)
[Fe(PPIX)F][e]	$^1/_2$	+26.7	2.91			
	$^3/_2$	+11.9	2.40			
	$^5/_2$	0.0	0.43	0.84		
[Fe(PPIX)Br][f]	$^1/_2$	+35.2	2.73			
	$^3/_2$	+13.5	1.99			
	$^5/_2$	0.0	0.36	0.91	0.75[g] (6 K)	5.94[h] (200 K)
[Fe(TPP)(NO_3)][i]	$^1/_2$	+37.3	1.79			
	$^3/_2$	+14.0	2.45			
	$^5/_2$	0.0	0.40	0.83		5.9[i] (258–303 K)
[Fe(PPIX)($SC_6H_4NO_2$)][j]	$^1/_2$	+28.3	1.35			
	$^3/_2$	+12.4	1.41			
	$^5/_2$	0.0	1.01	0.27	0.76[j] (4 K)	5.90[j] (295 K)
[Fe(OEP)(NCS)(Py)][k]	$^1/_2$	+18.3	3.44			
	$^3/_2$	+4.9	2.45			
	$^5/_2$	0.0	0.12	0.77		5.9[k] (77–299 K)
[Fe(TPP)($TMSO)_2$][+l]	$^1/_2$	+17.9	3.17			
	$^3/_2$	+4.5	3.27			
	$^5/_2$	0.0	1.12	0.10	1.22[m] (4 K)	6.05[l] (25 °C)
[Fe(TPP)($H_2O)_2$][+n]	$^1/_2$	+14.3	3.80			
	$^3/_2$	+0.5	4.63			
	$^5/_2$	0.0	1.32	0.03	1.53[n] (78 K) 1.69 (298 K)	5.6[n] (77–298 K)
[Fe(OEP)($C_2H_5OH)_2$][+o]	$^1/_2$	+17.1	2.56			
	$^3/_2$	−0.4	3.46	0.01	3.47[p] (4 K) 3.32 (115 K) 2.97 (295 K)	4.5[p] (295 K)
	$^5/_2$	0.0	1.46	0.04	1.89[q] (4 K)	5.9[q] (4–100 K)
Intermediate-Spin Complexes						
[Fe(TPP)(ClO_4)][r]	$^1/_2$	+25.1	3.26			
	$^3/_2$	0.0	3.20	0.30	3.50[s] (4 K) 3.16 (195 K) 2.79 (295 K)	4.5–5.3[r] (25 °C)
	$^5/_2$	+1.8	0.95			
[Fe(OEP)(3-ClPy)$_2$][+t] (monoclinic)	$^1/_2$	+17.2	3.44			
	$^3/_2$	0.0	3.14	0.08	2.7[t] (4 K) 2.52 (295 K)	3.7–4.7[t] (77–295 K)
	$^5/_2$	+2.8	1.02			
[Fe(OEP)($THF)_2$][+u]	$^1/_2$	+22.1	3.65			
	$^3/_2$	0.0	3.48	0.01	3.34[u] (4 K) 3.18 (298 K)	4.2–4.7[u] (77–275 K)
	$^5/_2$	+7.1	1.57			
Low-Spin Complexes						
[Fe(TPP)($CN)_2$][-v]	$^1/_2$	0.0	2.31	0.16	0.35[w] (4 K)	2.26[v] (21 °C)
	$^3/_2$	+22.4	3.59			
	$^5/_2$	+18.9	0.42			
[Fe(TPP)(CN)(Py)][x]	$^1/_2$	0.0	2.46	0.16	1.24[y] (4 K)	2.6[x] (25 °C)
	$^3/_2$	+22.6	3.39			
	$^5/_2$	+19.0	0.51			
[Fe(TPP)($Py)_2$][+z]	$^1/_2$	0.0	2.71	0.37	1.95[aa] (4 K)	2.2–2.9[bb] (200–320 K)
	$^3/_2$	+11.4	2.35			
	$^5/_2$	+16.3	0.23			
[Fe(TPP)(N_3)(Py)][cc]	$^1/_2$	0.0	2.19	0.12	2.25[dd] (4 K) 2.45[ee] (4 K)	2.09–2.33[cc] (77–297 K)
	$^3/_2$	+12.3	1.21			
	$^5/_2$	+12.2	0.85			
[Fe(OEP)(3-ClPy)$_2$][+ff] (triclinic at 98 K)	$^1/_2$	0.0	2.46	0.58	2.10[t] (4 K) 2.08 (295 K)	2.7[ff] (77 K)
	$^3/_2$	+7.7	2.21			
	$^5/_2$	+9.6	0.28			
[Fe(TPP)(NCS)(Py)][k]	$^1/_2$	0.0	2.39	0.67		3.04–3.67[k] (77–295 K)
	$^3/_2$	+7.4	2.23			
	$^5/_2$	+9.4	0.37			

[a] Reference 18. [b] [Fe(TPP)Cl], ref 36. [c] [Fe(TPP)Cl], ref 42. [d] Reference 19. [e] Reference 20. [f] Reference 21. [g] [Fe(TPP)Br], ref 36. [h] [Fe(TPP)Br], ref 42. [i] Reference 22. [j] Reference 23. [k] Reference 24. [l] Reference 25. [m] [Fe(TPP)($Me_2SO)_2$]$^+$, ref 25. [n] Reference 26. [o] Reference 27. [p] [Fe(OEP)](ClO_4)($EtOH)_2$, ref 38. [q] [Fe(TPP)($EtOH)_2$]$^+$, ref 37. [r] Reference 28. [s] Reference 40. [t] Reference 29. [u] Reference 30. [v] Reference 31. [w] [Fe(PPIX)($CN)_2$]$^-$, ref 41. [x] Reference 32. [y] [Fe(PPIX)(CN)(Py)], ref 41. [z] Reference 33. [aa] [Fe(PPIX)($Py)_2$]$^+$, ref 41. [bb] [Fe(OEP)($Py)_2$]$^+$, ref 43. [cc] Reference 34. [dd] CCP-N_3, ref 41. [ee] MMB-N_3, ref 41. [ff] Reference 35. [gg] The numerical value of the quadrupole splitting ΔE_Q in mm/s is obtained from the relation $\Delta E_Q = 10.12\delta(1 - R)Qq(1 + \eta^2/3)^{1/2}$, where the electric field, q, is in au and the constants Q, R, and δ are given in the text.

Table II. Mulliken Closed-Shell (Open-Shell) Populations[a] for the Iron d Orbitals in the High-, Intermediate-, and Low-Spin Ferric Complexes

compound	d_{z^2}	$d_{x^2-y^2}$	d_{xy}	d_{xz}	d_{yz}
		High-Spin Complexes			
[Fe(C_2-Cap)Cl]	0.65 (0.67)	0.56 (0.71)	0.02 (0.99)	0.10 (0.95)	0.10 (0.95)
[Fe(PPIX)Cl]	0.67 (0.66)	0.55 (0.72)	0.02 (0.99)	0.10 (0.95)	0.10 (0.95)
[Fe(PPIX)F]	0.44 (0.76)	0.57 (0.71)	0.02 (0.99)	0.13 (0.94)	0.12 (0.94)
[Fe(PPIX)Br]	0.55 (0.71)	0.55 (0.72)	0.02 (0.99)	0.10 (0.95)	0.10 (0.95)
[Fe(TPP)(NO_3)]	0.45 (0.77)	0.56 (0.72)	0.02 (0.99)	0.17 (0.91)	0.15 (0.92)
[Fe(PPIX)($SC_6H_4NO_2$)]	0.75 (0.61)	0.54 (0.73)	0.02 (0.99)	0.10 (0.95)	0.10 (0.95)
[Fe(OEP)(NCS)(Py)]	0.57 (0.71)	0.56 (0.71)	0.02 (0.99)	0.08 (0.96)	0.08 (0.96)
$[Fe(TPP)(TMSO)_2]^+$	0.35 (0.82)	0.67 (0.66)	0.02 (0.99)	0.08 (0.96)	0.08 (0.96)
$[Fe(TPP)(H_2O)_2]^+$	0.33 (0.83)	0.75 (0.62)	0.02 (0.99)	0.10 (0.95)	0.09 (0.95)
$[Fe(OEP)(C_2H_5OH)_2]^+$	0.30 (0.84)	0.73 (0.63)	0.03 (0.99)	0.09 (0.95)	0.10 (0.95)
		Intermediate-Spin Complexes			
[Fe(TPP)(ClO_4)]	0.29 (0.83)	0.67 (0.00)	1.99 (0.01)	0.08 (0.96)	0.09 (0.95)
$[Fe(OEP)(3\text{-}ClPy)_2]^+$ (monoclinic)	0.31 (0.83)	0.68 (0.00)	1.96 (0.02)	0.10 (0.95)	0.07 (0.96)
$[Fe(OEP)(THF)_2]^+$	0.22 (0.88)	0.70 (0.00)	1.99 (0.00)	0.09 (0.95)	0.08 (0.95)
		Low-Spin Complexes			
$[Fe(TPP)(CN)_2]^-$	0.70 (0.00)	0.46 (0.00)	1.98 (0.00)	0.98 (0.49)	1.04 (0.46)
[Fe(TPP)(CN)(Py)]	0.68 (0.00)	0.51 (0.00)	1.98 (0.00)	1.53 (0.22)	0.51 (0.73)
$[Fe(TPP)(Py)_2]^+$	0.56 (0.00)	0.56 (0.00)	1.96 (0.00)	1.57 (0.20)	0.49 (0.75)
[Fe(TPP)(N_3)(Py)]	0.63 (0.00)	0.50 (0.00)	1.98 (0.00)	0.79 (0.59)	1.32 (0.33)
$[Fe(OEP)(3\text{-}ClPy)_2]^+$ (triclinic at 98 K)	0.54 (0.00)	0.56 (0.00)	1.96 (0.01)	0.81 (0.59)	1.25 (0.38)
[Fe(TPP)(NCS)(Py)]	0.53 (0.00)	0.54 (0.00)	1.94 (0.02)	0.99 (0.50)	1.11 (0.43)

[a] Total orbital electron density is the sum of the closed-shell and open-shell populations.

Table III. Net Charges and (Unpaired Spins) on Fe, Axial Ligands, and Porphyrin in the High-, Intermediate-, and Low-Spin Ferric Complexes

compound	Fe	L_1[a]	L_2[a]	porph
		High-Spin Complexes		
[Fe(C_2-Cap)Cl]	1.35 (4.31)	−0.79 (0.17)		−0.56 (0.52)
[Fe(PPIX)Cl]	1.36 (4.31)	−0.79 (0.19)		−0.57 (0.50)
[Fe(PPIX)F]	1.29 (4.38)	−0.64 (0.14)		−0.65 (0.49)
[Fe(PPIX)Br]	1.21 (4.37)	−0.62 (0.12)		−0.59 (0.51)
[Fe(TPP)(NO_3)]	1.25 (4.34)	−0.60 (0.12)		−0.65 (0.54)
[Fe(PPIX)($SC_6H_4NO_2$)]	1.23 (4.28)	−0.62 (0.17)		−0.61 (0.55)
[Fe(OEP)(NCS)(Py)]	1.29 (4.34)	−0.68 (0.11)	0.14 (0.03)	−0.75 (0.52)
$[Fe(TPP)(TMSO)_2]^+$	1.38 (4.40)	0.16 (0.10)	0.16 (0.10)	−0.54 (0.50)
$[Fe(TPP)(H_2O)_2]^+$	1.26 (4.35)	0.19 (0.04)	0.19 (0.04)	−0.64 (0.57)
$[Fe(OEP)(C_2H_5OH)_2]^+$	1.35 (4.37)	0.15 (0.04)	0.15 (0.04)	−0.65 (0.55)
		Intermediate-Spin Complexes		
[Fe(TPP)(ClO_4)]	1.16 (2.78)	−0.75 (0.05)		−0.41 (0.17)
$[Fe(OEP)(3\text{-}ClPy)_2]^+$ (monoclinic)	1.21 (2.77)	0.18 (0.05)	0.18 (0.05)	−0.57 (0.13)
$[Fe(OEP)(THF)_2]^+$	1.30 (2.80)	0.12 (0.02)	0.12 (0.02)	−0.54 (0.16)
		Low-Spin Complexes		
$[Fe(TPP)(CN)_2]^-$	1.55 (0.95)	−0.81 (0.00)	−0.81 (0.00)	−0.93 (0.05)
[Fe(TPP)(CN)(Py)]	1.48 (0.95)	−0.74 (0.00)	0.14 (0.00)	−0.89 (0.03)
$[Fe(TPP)(Py)_2]^+$	1.37 (0.96)	0.21 (0.00)	0.21 (0.00)	−0.79 (0.04)
[Fe(TPP)(N_3)(Py)]	1.30 (0.92)	−0.53 (0.05)	0.16 (0.00)	−0.93 (0.03)
$[Fe(OEP)(3\text{-}ClPy)_2]^+$ (triclinic at 98 K)	1.32 (0.97)	0.21 (0.00)	0.21 (0.00)	−0.73 (0.03)
[Fe(TPP)(NCS)(Py)]	1.32 (0.95)	−0.68 (0.00)	0.17 (0.00)	−0.81 (0.05)

[a] L_1 and L_2 refer to the axial ligands in the order shown in the compound formula.

five-coordinate complexes. The net effect of the increase in the $d_{x^2-y^2}$ interaction with the porphyrin and the decrease in the d_{z^2} interaction with the axial ligands is an increase in the energy separation between the d_{z^2} and the $d_{x^2-y^2}$ orbitals, which results in the enhanced stability of the $S = {}^3/_2$ spin state in the six-coordinate complexes.[6]

The crystal structures of $[Fe(TPP)(TMSO)_2]^+$ and [Fe(OEP)(NCS)Py] are both examples of rarely obtained six-coordinate complexes exhibiting pure high-spin properties as indicated by their observed effective magnetic moments.[24,25] Our calculated value of ΔE_Q for $[Fe(TPP)(TMSO)_2]^+$ is in good agreement with the observed value of 1.22 mm/s for the $[Fe(TPP)(Me_2SO_2)]^+$ complex.[25] The isothiocyanate complex is very interesting in that, in addition to a high-spin [Fe(OEP)(NCS)Py] complex, a low-spin crystal structure of it with different porphyrin substituents, [Fe(TPP)(SCN)Py], has been synthesized,[24] which is also included and discussed in the present study. The high-spin complex exhibits calculated orbital populations resembling those of the five-coordinate complexes, which is not surprising since the crystal structure of this compound is very similar to that of a five-coordinate complex. That is, the iron atom is 0.24 Å out of the pyrrole nitrogen's plane, and its distance to the isothiocyanate and pyridine ligands is 2.03 and 2.44 Å, respectively.[24] The iron–pyridine distance is probably too long to significantly perturb the electronic structure of this essentially five-coordinate complex. In fact, the calculated ΔE_Q for this complex is the smallest for

the high-spin series, more resembling the calculated values for the five-coordinate complexes.

Our study indicates that the diaquo and diethanol complexes display significant deviations from the pure high-spin series in Table I and more closely resemble the intermediate-spin complexes. In the case of the diaquo complex, our results predict near-degenerate $S = {}^5/_2$ and ${}^3/_2$ states with the sextet state being slightly more stable. The measured value of the μ_{eff} for the reported crystal structure[26] is 5.6 μ_b over a temperature range 77–298 K. Additional determinations on other preparations[26] have also resulted in μ_{eff} = 5.5–5.7 μ_b at 298 K. These values are somewhat lower than the value of 5.9 μ_b for a pure high-spin complex. The anisotropic ESR g values are typical of predominantly high-spin mixed with a quartet state via spin–orbit coupling ($g \simeq 6$ and $g_\parallel \simeq 2$). The observed values of ΔE_Q for this complex are 1.53 and 1.69 mm/s at 78 and 298 K, respectively,[26] compared with calculated value of ΔE_Q = 1.32 mm/s for the sextet state. In view of our results, the observed properties of the diaquo complex can best be interpreted in terms of a dominant sextet ground state with significant quantum mixing from the quartet state.

The diethanol complex presents a more enigmatic situation. Dolphin et al.[38] have reported a μ_{eff} value of 4.5 μ_b (295 K) and ΔE_Q values of 2.97 mm/s (295 K) to 3.47 mm/s (4.2 K) for a Fe(OEP)ClO_4–2EtOH complex. On the basis of the large values of ΔE_Q and the observation of narrow-line symmetric doublets at all temperatures, they have assigned a $S = {}^3/_2$ single-spin ground state for this complex with no thermally induced spin crossover. The crystal structure of the ethanol solvate, [Fe(OEP)-$(EtOH)_2$]ClO_4·EtOH, which has been used in this study, has been interpreted[27] as high spin on the basis of equatorial ligand distances in the structure data. In another study[37] of a $[Fe(TPP)(EtOH)_2]^+$ complex in which structure was determined g values of $g \simeq 6$ and $g_\parallel \simeq 2$, μ_{eff} = 5.9 μ_b and ΔE_Q = 1.89 mm/s were reported, which are characteristic of a predominantly $S = {}^5/_2$ spin-mixed state. Finally, Mitra et al.[39] have reported ΔE_Q of 1.98 mm/s (77 K) and μ_{eff} values of 5.2 μ_b (80–293 K) and 3.6 μ_b (3.5 K) for yet another Fe(TPP)(ClO_4)·2(EtOH) + ${}^1/_2CH_2Cl_2$ complex, which they have interpreted as a spin-mixed ground state with predominantly $S = {}^5/_2$ character.

Our calculation for the $[Fe(OEP)(EtOH)_2]$ complex results in a ground quartet state with a near-degenerate sextet state for the crystal geometry[27] used. The calculated ΔE_Q's are 1.46 and 3.46 mm/s for the $S = {}^5/_2$ and $S = {}^3/_2$ states, respectively, both in agreement with the values reported for the high-[37,39] and the intermediate-spin[38] ground states of such a complex. Our results indicate that, contrary to the inference made from structural data[27] and in agreement with Dolphin's conclusion,[38] the crystal geometry used in our calculations corresponds to a dominant $S = {}^3/_2$ ground state, with significant quantum mixing from a sextet state. Unfortunately, magnetic data on this particular structure are not available for comparison because of crystal instability.[27] Although we have not explicitly calculated the spin states of the $[Fe(TPP)(EtOH)_2]^+$ complex, for lack of complete crystal geometry information,[37] it is likely that, on the basis of our isothiocyanate results (vide infra), the porphyrin substituents in this complex may impose axial ligand geometries that would lead to the stabilization of the sextet state. Independent of which spin state is the dominant ground state for a particular geometry, the near degeneracy of the calculated energies indicates that a significant mixing of these states is responsible for the observed magnetic properties. Since the extent of spin–orbit coupling varies inversely with the energy separation, nearly degenerate states would be expected to have significant spin mixing. These spin-mixed states could also, in principle, be present in a thermal equilibrium distribution. However, the absence of two sets of quadrupole-split doublets in the temperature-dependent Mössbauer spectra argues against significant thermal population of more than one state.[38]

Intermediate-Spin Complexes. Table I shows that, for the three formally intermediate-spin complexes considered, the $S = {}^3/_2$ state is the lowest in energy followed by the $S = {}^5/_2$ and $S = {}^1/_2$ states, respectively. The calculated energies of the doublet spin states are at least 17 kcal/mol above that of the quartet states. Therefore, a doublet contribution to the ground-state electronic and magnetic properties should be negligible. On the other hand, the calculated quartet states of [Fe(TPP)(ClO_4)] and [Fe-(OEP)(3-ClPy)$_2$]$^+$ are only 1.8 and 2.8 kcal/mol more stable than their respective sextet states. The bistetrahydrofuran complex, with a quartet–sextet energy difference of ~7 kcal/mol, exhibits the most stable $S = {}^3/_2$ ground state among the three complexes.

Our calculated results are consistent with and account for the observed magnetic susceptibility and electron spin resonance measurement of both [Fe(TPP)ClO_4][28] and mono-[Fe(OEP)(3-ClPy)$_2$][29] complexes and indicate closely lying quartet and sextet states. Magnetic susceptibility measurements of [Fe(TPP)(ClO_4)] yielded μ_{eff} values of 4.5–5.3 μ_b at 25 °C.[28] The ESR g and $g_\parallel$ values for this complex are 4.75 and 2.03, respectively. Similarly, μ_{eff} for $[Fe(OEP)(3\text{-}ClPy)_2]^+$ is 3.7–4.7 μ_b in the temperature range 77–294 K, and the g and $g_\parallel$ values are 4.92 and 1.97, respectively.

The Mössbauer spectra of both complexes exhibit single quadrupole doublets in zero magnetic field at all temperatures.[28,29,38] This behavior is indicative of the contribution of only one electronic state,[38] which could be spin mixed by interaction with other low-lying spin states, which do not, however, have appreciable population in thermal equilibrium. Our calculated ΔE_Q's are in very good agreement with the assignment[28,29,38,40] of $S = {}^3/_2$ as the ground state of these complexes. A triclinic form of $[Fe(OEP)(3\text{-}ClPy)_2]^+$ is found to be low spin, which is also correctly predicted by our calculations as discussed later.

The calculated energy difference of 7 kcal/mol between the sextet and quartet states of tetrahydrofuran complex predicts that the ground state of this complex should be a pure $S = {}^3/_2$ spin state. This is in agreement with the calculated ΔE_Q for this state. However, the observed μ_{eff} values of 4.2–4.7 μ_b in the temperature range 77–275 K and the g value of 4.61 at 77 K[30] are larger than those expected for a pure $S = {}^3/_2$ state and may indicate contribution from a low-lying $S = {}^5/_2$ state. In view of the reasonable predictions of the stability trends for all complexes studied here, the calculated 7 kcal/mol energy difference between the quartet and sextet states makes the possibility of thermal equilibrium between the two states unlikely in this complex. On the other hand, this value is not too much larger than the calculated energy differences between the sextet and quartet states of the high-spin, six-coordinate complexes, and the possibility of quantum mixing in tetrahydrofuran cannot be precluded.

It is generally accepted that the conditions for favoring an intermediate spin in a complex are weaker axial ligand and stronger in-plane ligand interactions with the iron d_{z^2} and $d_{x^2-y^2}$ orbitals.[6,53] However, comparison of the calculated closed-shell populations, in Table II, between the intermediate-spin and the six-coordinate, high-spin complexes does not reflect any pronounced variation arising from the interaction of the equatorial ligands with the $d_{x^2-y^2}$ orbital. This indicates that the assignment of spin state purely on the basis of equatorial ligand distances alone, as may be made from the structure data,[27] is not necessarily sufficient to distinguish between high- and intermediate-spin states.

The closed-shell d_{z^2} populations of [Fe(TPP)(ClO_4)] and $[Fe(OEP)(3\text{-}ClPy)_2]^+$ are similar to those of six-coordinate diaquo and diethanol complexes. This is consistent with the fact that the interaction of sextet and quartet states is important in all these complexes. The bistetrahydrofuran complex exhibits the weakest d_{z^2} axial ligand interaction, consistent with the rather pure $S = {}^3/_2$ spin state predicted for this complex.

As shown in Table III, the spin delocalization from the iron to the ligands and the porphyrin in the intermediate-spin compounds is considerably less (~0.2 e) than in the high-spin compounds (~0.7 e). Correspondingly, there is also much less unpaired spin on the porphyrin ring. Since most of the porphyrin unpaired spin is localized on the pyrrole nitrogens, the intermediate-spin complexes are expected to display less hyperfine splitting than the high-spin complexes.

Low-Spin Complexes. As shown in Table I, the calculated $S = {}^1/_2$ states are the lowest energy states in all formally low-spin

complexes investigated. Indeed, the ordering of the energy differences between either the sextet or the quartet state with the doublet state is roughly proportional to the combined field strength of the two axial ligands. For the first four low-spin complexes, the calculated energies of the higher multiplicity states are large enough that they are not expected to make any contribution to the $S = {}^1/_2$ ground state. This is in agreement with the observed magnetic moments,[31,32,34] which are typical of low-spin ferric complexes in a strong octahedral field.[34] Our calculated ΔE_Q's for these complexes are also typical of the low-spin values. However, they are in poor agreement with the reported values for dicyano and cyanopyridine ligands.[41] We believe that the reported values, obtained from the analysis of the spin Hamiltonian using crystal field parameters,[41] are anomalously low for these complexes. To our knowledge, ΔE_Q has not been reported for [Fe(TPP)(N_3)(Py)]. However, ΔE_Q values for the closely related azide complexes of metmyoglobin (MMB) and cytochrome *c* peroxidase (CCP) have been measured.[41] Although these complexes differ by one axial ligand, an imidazole instead of pyridine, the calculated value of 2.19 mm/s for the azopyridine complex is in good agreement with the experimental values[41] of 2.45 and 2.25 mm/s for CCP-N_3 and MMB-N_3, respectively.

Spin delocalization in these systems appears to be minimal, $\leq$0.05 e, with unpaired spin remaining in the d_{yz} and d_{xz} orbitals. The net charge on the iron is essentially the same in the low-spin complexes as it is in the high- and intermediate-spin complexes.

We have also calculated the spin states for the low-spin forms of the tri-[Fe(OEP)(3-ClPy)$_2$]$^+$ and [Fe(TPP)(NCS)(Py)] complexes using the frozen geometry of their appropriate crystal structures.[24,35] In both cases, the $S = {}^1/_2$ state is the lowest energy state, with the quartet and the sextet states about 7 and 9 kcal/mol higher in energy, respectively. The relatively stable low-spin states calculated for these complexes are in agreement with the typical low-spin magnetic moments observed for them.[29,35] The calculated ΔE_Q for tri-[Fe(OEP)(3-ClPy)$_2$]$^+$ is also in good agreement with its observed value.[29]

The calculated energy difference between the $S = {}^3/_2$ and $S = {}^5/_2$ states of tri-[Fe(OEP)(3-ClPy)$_2$]$^+$ is similar to that calculated in the case of the intermediate-spin monoclinic form of the complex. While the monoclinic complex is a predominantly $S = {}^3/_2$ admixture, the triclinic form is low spin at 98 K and a mixture of high and low spin at 293 K.[35] Our calculations of the triclinic form shows that, at the frozen low-temperature crystal geometry,[35] the $S = {}^1/_2$ is a single spin state, with minimal thermal or quantum mixing contributions from the higher spin states. This is in agreement with the observation[35] that the high-spin complex at room temperature has a different geometry than the low-spin crystal. However, change of the axial ligand distances to the reported high-spin values still results in a calculated quartet ground state. On the basis of the results for the intermediate-spin, monoclinic form and the close energies of $S = {}^5/_2$ and ${}^3/_2$ states, we can assert that, in the higher spin forms of this complex, whichever is the dominant spin state, the contributions from both $S = {}^3/_2$ and $S = {}^5/_2$ states are important. However, in its low-spin form, the doublet state is probably a pure spin state.

Finally, we have also calculated the relative energies of the spin states for the frozen geometry of the low-spin [Fe(TPP)(SCN)(Py)].[24] The low-spin state predicted for the complex is expected to be rather pure. The calculated ΔE_Q is also typical of a low-spin complex consistent with the magnetic data.[24]

Our use of frozen crystal geometry with porphyrin substituents replaced by hydrogens allows us to draw an important reference about the role of these substituents in determining the spin state. Our correct prediction of the spin states primarily from the geometries of the axial ligands and the porphyrin ring alone suggests that the porphyrin substituents have little direct electronic effects. Their role appears to be to modulate the geometry of the axial ligands either directly, i.e., by steric interaction, or indirectly, i.e., by affecting crystal packing parameters. The resulting ligand geometries then are one factor in determining the spin state of the complex.

Conclusions

We have quantitatively calculated the relative spin-state energies and the Mössbauer quadrupole splittings, ΔE_Q, for a large number of high-, intermediate-, and low-spin model ferric heme complexes, for which the crystal structures are known. The predicted spin state and the calculated energies of the other spin states relative to it are quantitatively consistent with experimentally observed electromagnetic properties for each of the complexes studied. The results are, therefore, both qualitatively and quantitatively sensitive to the type(s) and geometries of the axial ligand(s).

For all five-coordinate high-spin and six-coordinate low-spin complexes, for which unambiguous spin states have been assigned, our calculations also predict the correct ground spin state, with the other two spin states at much higher relative energies to have any significant interaction with the ground state. In general, six-coordinate high-spin complexes show a lowering of the sextet–quartet energy separation, indicating an enhanced interaction of $S = {}^5/_2$ and $S = {}^3/_2$ spin states. In the case of ferric complexes with diaquo or diethanol ligands, the sextet and quartet states become near degenerate. Therefore, while the exact $S = {}^5/_2$ or $S = {}^3/_2$ nature of the ground spin state may be sensitively dependent on geometry or other factors, the mixing of the two spin states, either thermally or through spin–orbit coupling, is evident.

Our calculated relative energies strictly correspond to pure spin states with no spin–orbit coupling interaction. They, therefore, cannot explicitly distinguish between thermal equilibrium or quantum admixture of the spin states. However, from the order of magnitude of the calculated energies and the experimental evidence, particularly Mössbauer spectra, we can infer that a quantum admixture, rather than thermal equilibrium, of $S = {}^3/_2$ and $S = {}^5/_2$ states is probably the prevalent mechanism for spin-state interactions in the complexes studied. This observation seems to be true for all complexes exhibiting predominantly intermediate or high spins.[54] We, thus, in contrast to previous reports,[43-47] find that contribution from the doublet state to more stable states of higher multiplicity or interaction of these states with a ground doublet to be negligible or minor in the complexes studied.

Our calculations, which are carried out for frozen crystal geometries, faithfully predict the spin states even in cases where different crystal geometries for the same two axial ligands lead to different spin states. Since porphyrin substituents were not included in our calculations, this indicates that they have little electronic effect, at least in these model compounds, on the spin state of the complex. The spin state is primarily determined by the type and the geometry of the axial ligands. Furthermore, the equatorial ligand distances alone are not sufficient to distinguish between a high- or an intermediate-spin state.

The model ferric heme calculations presented here indicate that the INDO/S-RHF method can be applied with confidence to characterize the spin state(s) of the heme active sites in intact proteins and enzymes, whenever the ligand types and geometries are known. Inversely, in the absence of such information, the axial ligand types and geometries can be inferred from comparison of the observed and predicted electromagnetic properties of various intermediates in the enzymatic cycle of a given enzyme.

We are grateful for the financial support of the National Science Foundation (Grant PCM 8410244) which made this work possible. We also thank the National Science Foundation for a supplement to the grant for generous use of the San Diego Supercomputer Center Class VI computers. The helpful guidance and support of the SDSC staff is also gratefully acknowledged.

(54) Ake, R. L.; Loew, G. M. H. *J. Chem. Phys.* **1970**, *52*, 1098.